THE JOURNAL OF PHYSICAL CHEMISTRY B

Article

pubs.acs.org/JPCB

Human Telomeric RNA G-Quadruplex Response to Point Mutation in the G-Quartets

Prachi Agarwala,[†,‡] Santosh Kumar,[‡] Satyaprakash Pandey,[†,‡] and Souvik Maiti*[,†,‡,§]

[†]Academy of Scientific and Innovative Research (AcSIR), Anusandhan Bhawan, 2 Rafi Marg, New Delhi 110001, India

[‡]Proteomics and Structural Biology Unit, CSIR-Institute of Genomics and Integrative Biology, Mall Road, New Delhi 110 007, India

[§]CSIR-National Chemical Laboratory, Dr. Homi Bhabha Road, Pune 411008, India

Supporting Information

ABSTRACT: Many putative G-quadruplex forming sequences have been predicted to exist in the human genome and transcriptome. As these sequences are subject to point mutations or SNPs (single nucleotide polymorphisms) during the course of evolution, we attempt to understand impact of these mutations in context of RNA G-quadruplex formation using human telomeric RNA (TERRA) as a model sequence. Our studies suggest that G-quadruplex stability is sensitive to substitution of the guanines comprising G-quartets. While central G-quartet plays a crucial role in maintaining the DNA G-quadruplex stability as evident in literature, there is equal importance of three G-quartets in the stability of RNA quadruplex structure. The work here highlights the alterations in the G-quartet are detrimental to the integrity of overall RNA G-quadruplex structure. Furthermore, TmPyP4 molecules are shown to exhibit similar binding behavior toward telomeric RNA G-quadruplex harboring base substitutions employing CD titrations and isothermal titration calorimetry; well indicating that mutation does not influence TmPyP4 recognition ability as it affects the stability of RNA G-quadruplex. Thus, our study implicates that mutation in G-quartets causes destabilization of RNA G-quadruplex without affecting its trans factor binding ability.

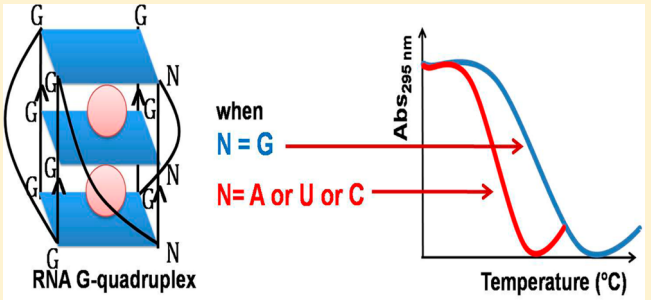

INTRODUCTION

G-quadruplexes are noncanonical secondary structures formed in G-rich sequences of nucleic acids.[1] Reports show widespread occurrences of putative G-quadruplex forming sequences across the human genome and transcriptome.[2−4] Classically, the putative G-quadruplex sequence has strategically placed guanine nucleotides forming G-quartets and interspersed nucleotides forming loop regions to allow for sufficient stereometric freedom. The above-described putative G-quadruplex site is represented by the sequence $G_{3+}N_{1-7}G_{3+}N_{1-7}G_{3+}N_{1-7}G_{3+}$, where G refers to guanine and N refers to any nucleotide other than guanine. Recently, alternate DNA G-quadruplex structures are reported where a nucleotide interrupting first guanine and next two guanines can form a bulge and project out of G-quartet core. Alternatively, a G-quadruplex can form when an isolated guanine residue present outside the stretch of consecutive guanines fold back to form the missing part of the incomplete G-tract. With variations and polymorphisms in the human genome, it is conceivable that SNPs (single nucleotide polymorphisms) may coincide in these sites which in turn can deviate the usual structure forming capacity from normalcy. Given sensitivity of G-quadruplex structures to the sequence composition, it becomes imperative to understand the sequence rules that govern the formation of quadruplex. In this purview, in depth-study on the differentially placed point mutations is prerequisite.

Several independent studies have demonstrated the effect of varying loop lengths and composition on the stability of G-quadruplexes at both DNA and RNA level.[5−15] Our group have demonstrated that not merely loop-length, the loop composition is also crucial for stability of RNA G-quadruplex.[16] Few other studies also are in concord with importance of loop length and composition on RNA G-quadruplexes stability.[16−18] However, there is no report investigating the consequences of base substitutions in the quartets of RNA G-quadruplexes. Although studies on mutations affecting the quartets of DNA G-quadruplexes do exist,[19−21] there is a need to perform a comprehensive study on the base substitutions in G-quartets of RNA G-quadruplex. RNA G-quadruplex is more thermodynamically stable and less hydrated compared to its DNA counterpart.[22] A comparison of different base substitutions' effects in the quartets of the RNA quadruplex is required to understand the tolerability of different base changes in the quartets.

Here, we aim to understand and draw meaningful comparisons when different bases are substituted for guanines comprising the quartets in RNA G-quadruplexes. We have taken the quadruplex forming 21 mer human telomeric repeat

Received: January 21, 2015
Revised: March 10, 2015

DOI: 10.1021/acs.jpcb.5b00619
J. Phys. Chem. B XXXX, XXX, XXX−XXX

Table 1. RNA Oligonucleotides Used for the Study

oligo name	sequence																				
TERRA	G	G	G	U	U	A	G	G	G	U	U	A	G	G	G	U	U	A	G	G	G
G4A TERRA	G	G	G	U	U	A	A	G	G	U	U	A	G	G	G	U	U	A	G	G	G
G5A TERRA	G	G	G	U	U	A	G	A	G	U	U	A	G	G	G	U	U	A	G	G	G
G6A TERRA	G	G	G	U	U	A	G	G	A	U	U	A	G	G	G	U	U	A	G	G	G
G4C TERRA	G	G	G	U	U	A	C	G	G	U	U	A	G	G	G	U	U	A	G	G	G
G5C TERRA	G	G	G	U	U	A	G	C	G	U	U	A	G	G	G	U	U	A	G	G	G
G6C TERRA	G	G	G	u	U	A	G	G	C	U	U	A	G	G	G	U	U	A	G	G	G
G4U TERRA	G	G	G	U	U	A	U	G	G	U	U	A	G	G	G	U	U	A	G	G	G
G5U TERRA	G	G	G	U	U	A	G	U	G	U	U	A	G	G	G	U	U	A	G	G	G
G6U TERRA	G	G	G	U	U	A	G	G	U	U	U	A	G	G	G	U	U	A	G	G	G

containing RNA (TERRA), substituted each of the three guanine residues of a G-tract with other three bases (adenine/cytosine/uracil) and then subjected them to structural and thermal analysis. We have also mutated residues in telomeric DNA G-quadruplex for comparison purpose. The telomeric sequence was deliberately chosen as the model system as it is well characterized for its sequence, structure, and thermal stability.[23] Additionally, NMR and crystal structures are already reported for the human telomeric G-quadruplex.[24−33] Furthermore, biophysical properties of human telomeric DNA and RNA G-quadruplex have been well studied and compared previously.[22] Thus, due to the availability of reference information, these sequences became our system of choice.

While studying the correlation between the positional effect of the base mutation and thermal stability of the resulting RNA G-quadruplex structure, we found that RNA G-quadruplex identity is effectively retained despite base changes; while huge changes in the thermal stability were recorded in UV melting experiments. We also compared the binding behavior of ligand TmPyP4 toward telomeric RNA G-quadruplex mutants. TmPyP4 is a known ligand against G-quadruplex and show two binding modes involving independent binding sites where it end stacks the G-quartets as well as interacts with loops of G-quadruplex.[12,22,34] We observed that binding behavior of TmPyP4 remains unchanged upon introducing mutations in quartets of G-quadruplex. On the basis of the biophysical behavior of telomeric G-quadruplex mutants, we conclude that contrary to more importance of middle quartet than end quartets in the overall DNA G-quadruplex structure, all three quartets are equally important for RNA G-quadruplex formation.

MATERIALS AND METHODS

Oligonucleotides and Chemicals. Oligonucleotides were procured from SBS Genetech and Sigma-Aldrich. Molar extinction coefficients were calculated with a nearest neighbor model as described before.[35] The concentrations of these oligonucleotides were calculated by recording the UV absorbance and by using their molar extinction coefficient values. The native sequence and the mutated sequences are given in Table 1 and Table S2 (Supporting Information). Sequences are given in the 5′ to 3′ direction.

5,10,15, 20-Tetrakis (1-methyl-4-pyridyl)- 21*H*,23*H* porphine (TmPyP4) was purchased in the form of tetra-*p*-tosylate salt from Sigma (USA).

CD Spectroscopy. A 5 μM sample of oligonucleotides prepared in 10 mM sodium cacodylate buffer with 100 mM KCl was heated at 95 °C and then allowed to slowly cool to 20 °C. CD spectra were recorded in Jasco spectropolarimeter (model 815, Japan) equipped with a thermoelectrically controlled cell holder and a quartz cuvette with a path length of 1 cm. CD spectra of the samples were recorded between 220 and 350 nm at 20 °C in 10 mM sodium cacodylate buffer (pH 7.4) with 100 mM KCl and each spectra is the average of three scans.

UV Melting Experiments. UV experiments were performed using Cary 100 (Varian) UV−vis spectrophotometer. Five μM of oligonucleotides were prepared in 10 mM sodium cacodylate buffer (pH 7.4) containing 100 mM KCl. The samples were heated at 95 °C and then allowed to slowly cool to 20 °C. Both heating and cooling profile of oligonucleotide was monitored at 295 nm at a rate of 0.2 °C/min. The absorbance values were converted to folded fraction by manually choosing upper and lower baselines. UV melting curves were analyzed using Mathematica version 5.0 and Origin version 7.0.

In cases where the system is in thermal equilibrium as suggested by reversible heating and cooling profile, we performed van't Hoff analysis for the intramolecular system. Melting temperature (T_m) values were obtained from thermal curve representing the temperature at which the folded fraction (α) is 0.5. T_m values differed by ±1.0 °C. The absorbance values recorded at 295 nm were utilized to estimate the thermodynamic parameters (within 10% error). This method involved the contribution from pretransition and post-transition baselines and thermodynamic data was obtained using equations described previously.[22]

$$A_u = b_u + (m_u \times T) \tag{1}$$

$$A_l = b_l + (m_l \times T) \tag{2}$$

$$K_{eq} = \frac{(1-\alpha)}{\alpha} \tag{3}$$

$$A(T) = \alpha(A_u - A_l) + A_l \tag{4}$$

$$K_{eq} = \exp\left(\frac{\Delta G^\circ}{RT}\right) = \exp\left(\frac{\Delta H^\circ}{RT} + \frac{\Delta S^\circ}{R}\right) \tag{5}$$

A_u, A_l are linear equations for the upper and lower baselines, respectively, where b_u and b_l describe fitted parameters for the intercepts for the upper and lower baseline with m_u and m_l as their respective slopes. Keq indicates the equilibrium constant for the unstructured-structured transition for an intramolecular system and α stands for the folded fraction. $A(T)$ being the dependent variable is experimentally determined absorbance at

DOI: 10.1021/acs.jpcb.5b00619
J. Phys. Chem. B XXXX, XXX, XXX−XXX

each temperature (T). These equations were used to calculate van't Hoff enthalpy (ΔH_{vH}) and entropy (ΔS_{vH}).

In some cases, thermal curve cannot be utilized to calculate thermodynamic parameters because of hysteresis. Thus, kinetic analysis of the thermal curves was performed.[36] Using two-state model for the folding−unfolding process, the equilibrium between folded (F) and unfolded (UF) fraction of the oligonucleotides is represented as

$$\mathrm{UF} \overset{k_{on}}{\rightleftarrows} \mathrm{F} \tag{6}$$

where, k_{on} and k_{off} are association and dissociation rate constants of folding and unfolding process of oligonucleotides, respectively. Their values are obtained from melting and annealing curves using the following rate equation:

$$\frac{d(\mathrm{F})}{dt} = k_{on}[\mathrm{UF}] - k_{off}[\mathrm{F}] \tag{7}$$

The use of folded fraction (α) in eq 7 yields the following equations:

$$\frac{d(\alpha_h)}{dt} = k_{on}(1 - \alpha_h) - k_{off}(\alpha_h) \tag{8}$$

$$\frac{d(\alpha_c)}{dt} = k_{on}(1 - \alpha_c) - k_{off}(\alpha_c) \tag{9}$$

where α_h and α_c are the folded fractions of nucleic acids at any temperature in the heating and cooling curve, respectively. In addition, $d(\alpha_h)/dt$ and $d(\alpha_c)/dt$ can be determined from eq 10, where dT/dt stands for the temperature gradient used during melting and cooling experiments and $d\alpha/dT$ is the term determined from the experimental melting and cooling curves.

$$\frac{d(\alpha)}{dt} = \frac{d\alpha}{dT} \times \frac{dT}{dt} \tag{10}$$

Equation 8 and eq 9 were solved to obtain the values of k_{on} and k_{off} at a wide range of temperatures. The temperature at which $k_{on} = k_{off}$ represents the T_m value.

Subsequently, activation energy (E_a) is determined using Arrhenius equation:

$$k = Ae^{-E_a/RT} \tag{11}$$

Here A is the frequency factor. Equation 11 is converted into the equation

$$\ln(k) = -\frac{E_a}{R}\left(\frac{1}{T}\right) + \ln(A) \tag{12}$$

Using the above Arrhenius equation, a plot of $\ln(k)$ versus $1/T$ was drawn where $(-E_a/R)$ and $\ln(A)$ terms symbolize the slope and y-intercept, respectively.

Furthermore, thermodynamic values were estimated on the basis of kinetic parameters. Enthalpy change (ΔH) was calculated from the equation: $\Delta H = E_{on} - E_{off}$, where E_{on} and E_{off} refers to the activation energy for association and activation energy for dissociation, respectively. The Gibb's energy change (ΔG) is calculated at 37 °C using the relation: $\Delta G = -RT \ln(K_a)$, where R, T, and K_a denote universal gas constant, absolute temperature and equilibrium constant, respectively. Finally, entropy change (ΔS) is calculated using equation: $\Delta G = \Delta H - T\Delta S$.

To test the accuracy of kinetic analysis, UV melting of G4A TERRA, G5A TERRA, and G6A TERRA oligonucleotides were also performed at the rate of 0.5 °C/min.

CD Titrations. Subtracting buffer alone, CD scans of 5 μM samples were taken at wavelength 220−350 nm at 20 °C. The samples were titrated against increasing concentration of TmPyP4 porphyrin and CD scans were taken. Thereafter, a plot of normalized CD signals at 260 nm for RNA G-quadruplex versus TmPyP4 concentration was drawn.

Isothermal Titration Calorimetry. Isothermal titration calorimetry experiments were performed on a Microcal VP-ITC (Microcal, Inc.; Northampton MA). Titrations of TERRA and its mutants with TmPyP4 were carried out at 25 °C. Then, 10 μL aliquots of 125 μM TmPyP4 from a 280 μL capacity rotating syringe were injected into an isothermal sample chamber containing 1.5 mL of oligonucleotide at 5 μM concentration. This experiment was accompanied by the control experiment in which 125 μM TmPyP4 was injected into a buffer solution alone. The duration of each injection was 20 s and the delay between the injections was 180 s, the initial delay preceding the first injection was 300 s. Each injection generated a heat burst curve (microcalories/second vs seconds) and the area under each curve was determined by integration [using the origin version 7.0 software (Microcal, Inc., Northampton, MA)] to obtain the measure of the heat associated with that injection. The buffer corrected ITC profiles for the binding of different oligonucleotides and TmPyP4 was fit with either a model for two set of binding sites or one set of binding.[37,38] The net enthalpy changes for G-quadruplexes with TmPyP4 were determined by subtraction of the heat of dilution from each binding isotherm.

RESULTS

Mutants with Base Substitutions in Quartets Retains Ability To Form Parallel RNA G-Quadruplex. Circular dichroism is a widely used technique to understand the secondary structure of a macromolecule. We employed CD to comprehend the secondary structure of oligonucleotides. Figure 1 shows the CD spectroscopic profile of TERRA and its mutants with the molar ellipticity as a function of wavelength. CD spectrum of TERRA displayed a positive signal at 260 nm and a negative signal at around 240 nm of wavelength indicating formation of parallel G-quadruplex. CD spectra of all TERRA mutants similarly showed these signatures of parallel G-quadruplex. However, the intensity of peak at 260 nm in CD spectra of TERRA mutants showed 8−36% decrease relative to TERRA with G4C and G5A mutants showing minimum and maximum decrease, respectively.

Figure S1 (Supporting Information) shows CD profile of Telo DNA and its mutants. CD spectra of native wild type sequence shows maxima at 290 nm and minima at 258 nm in 10 mM sodium cacodylate buffer containing 100 mM KCl, which is typical spectra of antiparallel quadruplex. A negative peak at 233 nm is also observed indicating presence of a mixed population of predominantly antiparallel structure and less contributing parallel conformation. Interestingly, similar to the wild type sequence, the sequences containing quartet modifications also displayed spectra of a mixed structure comprising predominant antiparallel population and residual parallel population. This suggests that all sequences were able to fold into quadruplex regardless of base substitutions. However, intensities of peaks vary in sequences with different mutations. Thus, CD spectra of mutants of both TERRA and Telo DNA displayed signature of G-quadruplex but with varied peak intensities.

DOI: 10.1021/acs.jpcb.5b00619
J. Phys. Chem. B XXXX, XXX, XXX−XXX

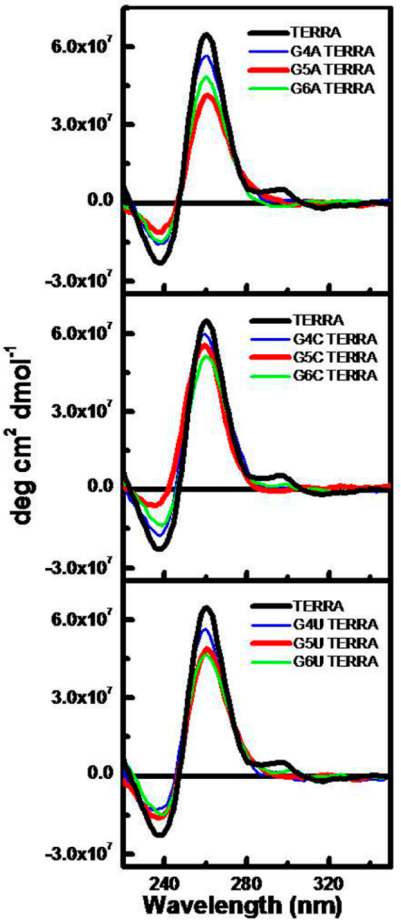

Figure 1. CD spectroscopic profile of RNA oligonucleotides with single Guanine to Adenine (top row), Cytosine (middle row), Uracil (bottom row) mutation in TERRA sequence: 5′-GGGUUAG(4)-G(5)G(6)UUAGGGUUAGGG-3′ sequence. Color codes for the traces are wild type (black), 4th position (blue), 5th position (red), and 6th position (green). Molar ellipticity as a function of wavelength is plotted. Sequences were buffered in 10 mM sodium cacodylate (pH 7.4) containing 100 mM KCl and spectra were taken at 20 °C.

Mutations in G-Quartets Destabilize RNA G-Quadruplex Considerably. Thermal stability of wild type and mutated TERRA sequences bearing single base substitutions of guanines residues were determined using UV spectroscopy. Figure 2 represents thermal melting profiles of all sequences performed at the rate of 0.2 °C/min. TERRA and its mutants showed hypochromic shift at 295 nm with increasing temperature, a characteristic signature of G-quadruplex.[39] TERRA displayed a Tm value of 77 °C in 10 mM sodium cacodylate containing 100 mM KCl. As annealing and melting curve were in equilibrium, the thermodynamic parameters were calculated from thermal curves. TERRA was found to be highly stable with ΔG value of −12.5 kcal/mol at 37 °C. UV profile of all TERRA mutants also showed hypochromic shift with increasing temperature, indicating their ability to form G-quadruplex even in the presence of mutations. However, significant reduction in thermal stability is observed upon introducing single nucleotide substitutions in the RNA G-quadruplex stem (Figure 2).

Unlike wildtype TERRA, the annealing and melting curves of TERRA mutants were not superimposable. Hysteresis was observed between these curves, indicating a difference in the rate of formation and denaturation of G-quadruplex. The apparent half-temperature for annealing ($T_{1/2\text{-anneal}}$) and melting ($T_{1/2\text{-melt}}$) were calculated from cooling and melting curve, respectively (Table 2). A difference of 1−6 °C was observed between $T_{1/2\text{-anneal}}$ and $T_{1/2\text{-melt}}$. The melting curve showed $T_{1/2\text{-melt}}$ value higher than annealing curve $T_{1/2\text{-anneal}}$ indicating slower rate of melting. Hysteresis was more pronounced in G6 mutants with half-temperature difference of 4.5−5.5 °C. However, in G4A mutant also, a half-temperature difference of 4.8 °C was observed between annealing and melting curves. On further examining the curves closely, we observed less hysteresis in G4C and G5C mutants compared to other mutants.

Because of hysteresis, the thermal curve of TERRA mutants could not be used directly for thermodynamic analysis. Therefore, kinetic analysis of folding and unfolding processes of RNA G-quadruplex was carried out. The kinetic analysis facilitates the determination of the activation energy (E_a), association rate constant (k_{on}) and dissociation rate constant (k_{off}) values. This kinetic analysis using two-state (all or none) model has been reported earlier for the duplexes as well as noncanonical structures.[36,40−42] The k_{on} and k_{off} values were estimated at various temperatures to determine the mechanisms of folding and unfolding processes. Upon analysis, k_{on} values were found to be higher (range of 27×10^{-4} to 1229×10^{-4} s) than k_{off} (range of 4×10^{-4} to 151×10^{-4} s) values at 37 °C in all mutants indicating the faster rate of folding than unfolding. This difference in association and dissociation rate is accountable for the hysteresis between cooling and melting curves. Association rate constants values varied for different TERRA mutants, clearly indicating vast differences in folding and unfolding rates in the presence of base substitutions at different positions. Subsequently, the Arrhenius plot of $\ln(k_{on})$ and $\ln(k_{off})$ versus $1/T$ was drawn. From the slope of these plots, the activation energy for folding (E_{on}) and unfolding (E_{off}) were estimated. These plots showed positive slope for k_{on} and negative slope for k_{off} indicating negative E_{on} values (−16.2 to −45.8 kcal/mol) and positive E_{off} values (13 to 30 kcal/mol) for all TERRA mutants, respectively.

On the basis of these kinetic parameters, the thermodynamic analysis was performed (Table 2). Gibb's free energy change (ΔG) at 37 °C was calculated for TERRA mutants. Formation of RNA G-quadruplexes was thermodynamically favorable with ΔG value in the range of 1.1−2.3 kcal/mol indicative of their stability at physiological temperature. The enthalpic stabilization of RNA G-quadruplex was consistent in each case. Although the G-quadruplex formation was entropically unfavorable, it was highly compensated by favorable enthalpy values. Among the TERRA mutants, ΔG values (−2.2 kcal/mol) of G4C mutant was found to be lowest. We also performed UV melting and annealing processes of three mutants- G4A TERRA, G4C TERRA, and G4U TERRA at a different rate, i.e., 0.5 °C/min, and determined kinetic and thermodynamic parameters (Table S1 in Supporting Information). We compared these parameters with those evaluated at the rate of 0.2 °C/min and found them to be similar; indicating our kinetic analysis of mutants' UV melting is accurate.

G-quadruplexes of TERRA mutants in comparison with wildtype TERRA demonstrated reduced stability. ΔG values of TERRA mutants were six times lower than TERRA (−12.5 kcal/mol). Moreover, for all types of base substitution (adenine/cytosine/uracil), ΔG values remained more or less similar. Irrespective of position, base substitution of any

DOI: 10.1021/acs.jpcb.5b00619
J. Phys. Chem. B XXXX, XXX, XXX−XXX

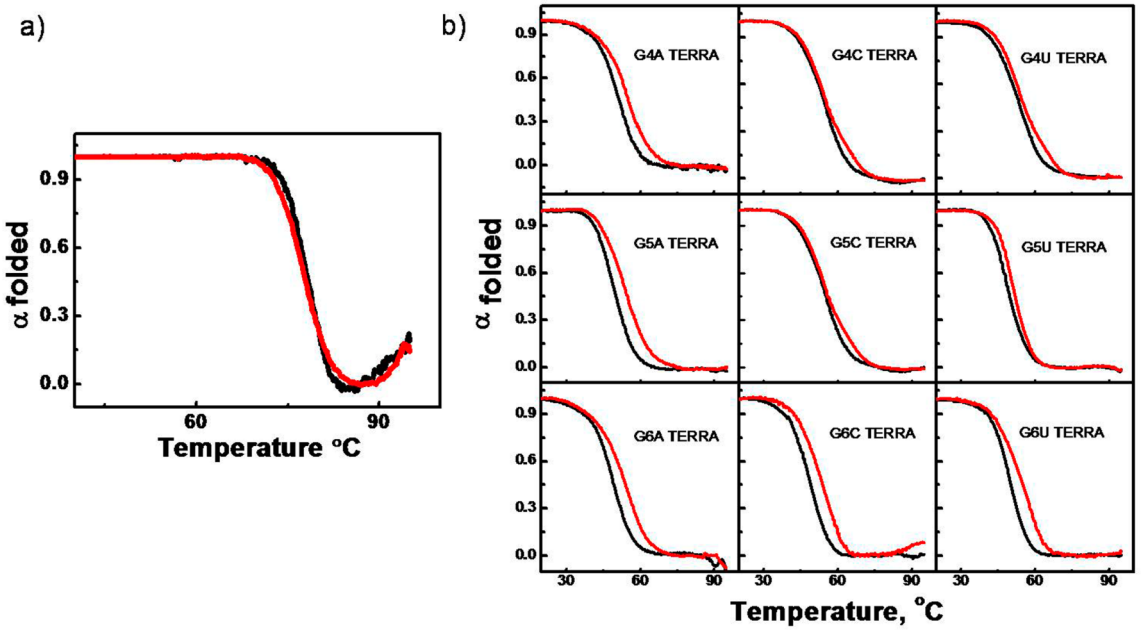

Figure 2. UV denaturation (red) and renaturation (black) profile of RNA oligonucleotides. (a) TERRA (b) TERRA mutants with single base substitutions of guanine (in bracket) to adenine (left column), cytosine (middle column), uracil (right column) in TERRA: 5′-GGGUUAG(4)G(5)G(6)UUAGGGUUAGGG-3′ sequence. Folded fraction as a function of temperature is plotted. Sequences were buffered in 10 mM sodium cacodylate (pH 7.4) containing 100 mM KCl, and melting and annealing processes were carried out at the rate of 0.2 °C/min.

guanine residue caused a marked reduction in magnitude of ΔG values of G-quadruplexes highlighting its importance in G-quadruplex structure.

Finally, the T_m value for TERRA mutants was evaluated. T_m corresponds to the temperature at which $k_{on} = k_{off}$. TERRA mutants showed T_m in range of 48−53 °C demonstrating 23−29 °C reduction in T_m value compared to unmodified TERRA. This clearly suggests that mutation in the G-quartets, irrespective of position and base type, caused conspicuous destabilization in G-quadruplex formation. Each of the guanine quartet mutations is detrimental for the formation of this RNA secondary structure.

Similarly, UV melting of Telo DNA and its mutants with single base substitutions was performed to determine their thermal stabilities. Unmodified Telo DNA and mutants gave hypochromic UV profile upon denaturation and renaturation. The annealing and melting curves were superimposable for Telo DNA and its mutants (except G5A Telo and G5C Telo). However, the stability of the structure is visibly reduced upon introduction of single nucleotide substitution mutations in the G-quartets (Table S3). There was a sharp drop in T_m value; by at least 10−12 °C and ranges up to 32 °C depending on the position of mutation in the nucleotide sequence. Base substitution of guanine residues constituting first and third G-quartets showed a ΔT_m of average 12 °C. The most striking destabilization profile was displayed by the mutations in the second quartet which brought down the T_m by 28 °C. Thus, there is quartet dependent pattern of ΔT_m variation.

Extended thermodynamic analysis showed that all of the mutated DNA G-quadruplexes are thermodynamically stable at physiological temperature. Table S3 represents the thermodynamic profile of individual sequences and shows that the negative entropy contribution to $\Delta G°$ is overridden by the large favorable enthalpy in all cases. Yet, a closer look at the profiles across the quartets shows that $\Delta G°$ values, though negative are very low in magnitude in case of mutations in the second quartet. The top and the bottom quartet mutations, in most cases, have relatively less effect on the individual $\Delta G°$ values.

Decrease in thermal stability was observed to be almost similar in different base substitutions and so was the thermodynamic profile. The guanines substituted with adenine or thymine showed a comparable decrease in the thermodynamic stability while in the case of substitution with cytosines, we observe slightly lower ΔT_m suggesting a less pronounced effect with cytosine substitution. Overall, we report a vastly position specific effect of single base mutations without much difference in the thermodynamic stability due to individual base composition.

Thus, in contrast to TERRA RNA G-quadruplex where the mutations in all G-quartets are equally harmful for its stability, the impact of mutations is unevenly distributed among G-quartets of Telo DNA G-quadruplex. Mutations in the middle G-quartet caused more pronounced destabilizing effect on Telo DNA G-quadruplex than first and third G-quartets. However, for both DNA and RNA G-quadruplexes, mutations were found to be detrimental irrespective of base substitution type.

TmPyP4 Binds Wildtype and Mutant RNA G-Quadruplex at Two Binding Sites. TmPyP4 is a known ligand for G-quadruplex. In order to understand the influence of mutations on ligand recognition ability, CD titrations were performed. Five μM of oligonucleotide was prepared and was titrated with increasing concentration of TmPyP4. CD titrations were performed until the final concentration of TmPyP4 in cuvette reached 25 μM. As evident in Figure 3, the intensity of peak at 260 nm of TERRA and its mutants decreased with increasing concentration of TmPyP4.

Then, normalized value of oligonucleotide at 260 nm was plotted against increasing concentration of TmPyP4 and mutants' plot was compared with TERRA plot. TmPyP4 binds with TERRA in 1:1 ratio at first binding site and 2:1 ratio at second binding site. Saturation in TmPyP4 binding site is achieved once 3:1 ratio of TmPyP4 and TERRA is reached.

DOI: 10.1021/acs.jpcb.5b00619
J. Phys. Chem. B XXXX, XXX, XXX−XXX

Table 2. Kinetic and Thermodynamic Parameters Obtained for TERRA and Mutant RNA Oligonucleotides from UV Melting Studies

oligo name	$T_{1/2\text{-melt}}$ (°C)	$T_{1/2\text{-anneal}}$ (°C)	hysteresis	E_{on} (kcal mol^{-1})	E_{off} (kcal mol^{-1})	k_{off} ($\times 10^{-4}$ s^{-1})	K_{on} ($\times 10^{-4}$ s^{-1})	K_a	ΔG (kcal mol^{-1})	ΔH (kcal mol^{-1})	$T\Delta S$ (kcal mol^{-1})	ΔS (cal mol^{-1})	T_m(°C)	ΔT_m(°C)
TERRA	77	77							−12.5	−108.3		−309.1		
G4A TERRA	52.9	48.1	4.8	−27.0	22.9	4.7	35.8	7.5	−1.2	−49.9	−48.7	−157.0	56.5	26 4
G5A TERRA	51.1	48.4	2.7	−38.1	14.8	9.2	156.3	16.9	−1.7	−52.9	−51.2	−165.1	49.9	27
G6A TERRA	51.6	46.4	5.2	−33.7	17.2	5.4	36.3	6.7	−1.2	−50.9	−49.7	−160.4	48.8	28.1
G4C TERRA	53.8	52.6	1.2	−31.9	13.0	30.2	1145.4	37.9	−2.2	−44.9	−42.7	−137.7	53.2	23.7
G5C TERRA	49.6	48.1	1.5	−32.9	22.9	151.8	1229.9	8.1	−1.3	−55.8	−54.5	−175.9	48.7	28.2
G6C TERRA	52.7	47.1	5.6	−45.8	28.7	2.7	27.8	10.3	−1.4	−50.1	−48.7	−157.0	49.6	27.3
G4U TERRA	52.9	51.1	1.8	−16.2	22.0	6.9	124.1	17.9	−1.8	−38.2	−36.5	−117.7	52.3	24.6
G5U TERRA	50.2	48.1	2.1	−25.9	30.1	33.8	263.4	7.8	−1.3	−56.0	−54.8	−176.7	48.7	28.2
G6U TERRA	53.2	48.6	4.6	−39.6	14.8	5.0	69.3	13.8	−1.6	−54.4	−52.8	−170.2	50.7	26.2

Kinetic and thermodynamic parameters for RNA G-quadruplex (5 μM) obtained from UV melting performed at the rate of 0.2 °C/min in 10 mM sodium cacodylate buffer (pH 7.4) containing 100 mM KCl. K_{on}, k_{off}, K_a, ΔH, ΔS, and ΔG values are calculated at 37 °C. Kinetic and thermodynamics parameters reported are within 10% error.

Figure 3. Normalized CD signal of RNA oligonucleotides at 260 nm is plotted against increasing concentration of porphyrin after performing CD titrations of RNA oligonucleotides with TmPyP4. Titrations were performed in 10 mM sodium cacodylate buffer (pH 7.4) containing 100 mM KCl.

With further addition of ligand molecules, slight changes in curve occur mainly due to the binding of TmPyP4 to the single stranded RNA. Similarly, TERRA mutants' plot shows saturation at 3:1 ratio of ligand and mutants. Thus, the stochiometry of TmPyP4 binding to TERRA mutants were found to be consistent with the native TERRA. This suggests that mutations in TERRA do not bring about major changes in the number of binding sites of TmPyP4 for RNA G-quadruplex.

TmPyP4 Binds Similarly with Wildtype and Mutant RNA G-Quadruplex. Isothermal titration calorimetry is a highly sensitive tool to directly and accurately measure the thermodynamic parameters of biological interactions. It is widely used to study binding behavior of a ligand toward a macromolecule. In a single experiment, it provides stoichiometry (n) and thermodynamics values of enthalpy and entropy.

Here, thermodynamic parameters were calculated by titrating TmPyP4 molecule against TERRA and its mutants. The concentration of oligonucleotides was kept constant in the cell and titrated with stepwise addition of TmPyP4 from the syringe. Titrations were performed until the ligand TmPyP4 was five times in excess of the oligonucleotide in the cell. The integrated heat data of G-quadruplex interactions with TmPyP4 are shown in Figure 4 and Figure S4, and corresponding thermodynamic data are given in Table 3. For most titrations,

DOI: 10.1021/acs.jpcb.5b00619
J. Phys. Chem. B XXXX, XXX, XXX−XXX

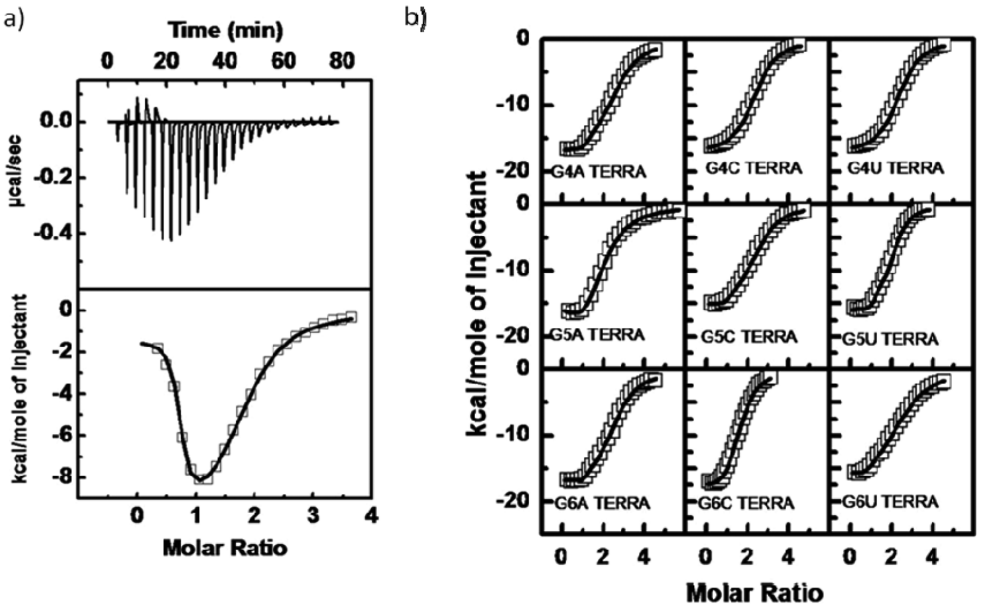

Figure 4. ITC isotherms of porphyrin with (a) TERRA and (b) TERRA mutants. ITC experiments were performed in 10 mM sodium cacodylate buffer (pH 7.4) containing 100 mM KCl.

the integrated heat data was biphasic depicting two modes of binding. The model with two binding modes involving two independent sites were used to fit the TmPyP4-quadruplex titration data as it gave the best fitting and high χ^2 value. The overall integrated heat profile for porphyrin titrations against TERRA mutants were similar in pattern whereas they moderately differed from that of native TERRA.

TmPyP4 showed two binding modes with wildtype TERRA. The two binding modes of TmPyP4 for RNA G-quadruplex differed in their binding affinity, with the first mode of binding affinity 2 orders of magnitude greater than second mode of binding affinity. The stochiometry for first and second binding modes were found to be 1 and 2 respectively. TmPyP4 retained two modes of binding with TERRA mutants harboring base substitutions in the G-quartets. Even the stoichiometry of binding was similar to that of wildtype TERRA. Except G6A mutant, TmPyP4 binding affinity is similar in wildtype TERRA and mutants. This suggests that base substitutions did not affect the strength of TmPyP4 binding to the RNA G-quadruplex. TmPyP4 displayed similar binding behavior to TERRA mutants irrespective of type and position of the base substitution.

The thermodynamic parameters of two binding modes of TmPyP4 for wildtype and modified TERRA sequences were compared. In TERRA, favorable enthalpy value was supported by highly favorable entropy value upon TmPyP4 binding to first binding site making ΔG value highly favorable. On the contrary, mutations in TERRA caused the enthalpy for TmPyP4 binding to become highly favorable and entropy to be unfavorable. Again, due to enthalpy−entropy compensation, the overall ΔG value became favorable. This is well represented in the heat profile of TmPyP4 titrations against TERRA and mutants (Figure 4 and Figure S4). The enthalpic values for second binding modes for both TERRA and mutants were negative indicating the exothermic interactions between TmPyP4-quadruplex. Again, the negative values of Gibb's free energy at second binding site suggest that TmPyP4 binding to G-quadruplex is highly favorable. In most cases, ΔH values at second binding site of wildtype TERRA and mutants are approximately similar while there was increase in its magnitude at first binding site. Thus, mutations in G-quartets show similar TmPyP4 binding behavior, unfavorable entropy at first binding site being the major cause for bringing ΔG value at par with that of wildtype TERRA.

DISCUSSION

Biophysical studies on TERRA and mutants were performed using CD and UV spectroscopy. TERRA displayed CD spectrum with a positive peak at 260 nm and a negative peak at 240 nm, well abiding with the already known RNA G-quadruplex parallel topology. Because of the presence of 2′ hydroxyl group, there are conformational constraints on guanine residues of ribonucleosides to attain *anti* conformation about the glycosidic bond and not to form *syn* conformation, a prerequisite for antiparallel G-quadruplex formation. TERRA mutants also displayed CD spectra with maxima at 260 nm and minima at 240 nm. Though intensity of CD signals diminished, mutants retain the overall G-quadruplex parallel topology. Furthermore, we compared the effect of mutations on DNA G-quadruplex. Telo DNA exhibited CD signature characteristic to hybrid population of parallel and antiparallel G-quadruplex. With slight variations in percentage of parallel and antiparallel subpopulation, Telo DNA mutants maintained the G-quadruplex structure with hybrid topology, well in agreement with previous study.[19] These observed changes in CD signal intensities can be well attributed to disturbance of the quartets arising due to disruption of the regular Hoogsteen bonding network of the quartets.

Interestingly, the major divergence in consequences of mutations in TERRA G-quadruplex formation was observed on performing UV melting studies. On recording the absorbance changes at 295 nm, the unmodified telomeric TERRA gave thermal stability at 77 °C in 10 mM sodium cacodylate buffer containing 100 mM KCl; the T_m value is well in accordance with studies reported earlier.[22] Mutations in any guanine residue of TERRA G-quadruplex caused substantial destabilization of RNA G-quadruplex. About 23−29 °C decrease in T_m values was observed upon individually mutating guanine residues of three G-quartets, clearly indicating that all

DOI: 10.1021/acs.jpcb.5b00619
J. Phys. Chem. B XXXX, XXX, XXX−XXX

Table 3. Thermodynamic Parameters Obtained from RNA G-Quadruplex and TmPyP4 Interactions Obtained from ITC Experiments at 25 °C

oligo name	n_1	K_{a1} ($\times 10^{-7}$ M^{-1})	ΔH_1 (kcal mol^{-1})	ΔS_1 (cal mol^{-1} K^{-1})	$T\Delta S_1$ (kcal mol^{-1})	ΔG_1 (kcal mol^{-1})	n_2	K_{a2} ($\times 10^{-5}$ M^{-1})	ΔH_2 (kcal mol^{-1})	ΔS_2 (cal mol^{-1} K^{-1})	$T\Delta S_2$ (kcal mol^{-1})	ΔG_2 (kcal mol^{-1})
TERRA	0.8	7.4 ± 2.3	−1.4 ± 0.2	31.3	9.3	−10.7	1.2	7.5 ± 0.8	−10.6 ± 0.1	−8.6	−2.6	−8.0
G4A TERRA	1.1	6.3 ± 4.4	−16.7 ± 0.1	−20.5	−6.1	−10.6	1.5	6.8 ± 0.4	−17.5 ± 0.7	−32.2	−9.5	−8
G4C TERRA	0.9	0.2 ± 0.2	−18.1 ± 25	−32.2	−9.5	−8.6	1.4	14 ± 29	−16.7 ± 0.5	−28.1	−8.3	−8.4
G4U TERRA	1.0	6.2 ± 4.4	−18.6 ± 1.7	−26.7	−7.9	−10.7	0.9	15 ± 1	−17.2 ± 0.1	−29.3	−8.7	−8.5
G5A TERRA	1.0	7.1 ± 6.1	−15.7 ± 0.2	−16.8	−5.0	−10.7	1.1	10 ± 4	−16.8 ± 0.6	−28.9	−3.6	−8.2
G5C TERRA	1.1	3.7 ± 1.7	−15.2 ± 0.1	−16.3	−4.8	−10.4	1.4	8.1 ± 0.4	−15.0 ± 0.5	−23.4	−6.9	−8.1
G5U TERRA	1.0	12 ± 5	−15.9 ± 0.1	−16.4	−4.8	−11.1	1.1	11 ± 1	−15.1 ± 0.2	−22.9	−6.8	−8.3
G6A TERRA	1.0	46 ± 10	−16.7 ± 0.1	−16.6	−4.9	−11.8	1.5	7.5 ± 0.4	−18.6 ± 0.3	−35.4	−105	−8.1
G6C TERRA	1.1	0.9 ± 0.2	−17.7 ± 0.2	−27.5	−8.1	−9.6	0.8	5.5 ± 0.3	−15.6 ± 3.7	−26.1	−7.7	−7.9
G6U TERRA	0.8	4.9 ± 3.9	−15.7 ± 0.1	−17.5	−5.2	−10.5	1.7	5.0 ± 0.2	−17.3 ± 0.5	−32.2	−9.5	−7.8

ITC experiments were performed in 10 mM sodium cacodylate buffer (pH 7.4) containing 100 mM KCl.

guanines in G-quartets are essential for RNA G-quadruplex stability and their mutation are highly intolerable. On the contrary, the effect of base changes in Telo DNA on the thermal stability is far reaching in case of second quartet as these sequences are severely destabilized with T_m change of 25 °C. This indicates a position specific dependence of sequences for DNA quadruplex stability, well in accordance with previous reports.[19] This maximum destabilization recorded in the case of middle quartet G5 Telo DNA sequences was irrespective of the base composition.

A closer look at the thermal profile of TERRA displayed superimposing nature of annealing and melting curves, suggesting equilibrium between the folding and unfolding processes. However, upon introducing mutations in TERRA sequence, a clear hysteresis between UV melting and cooling curves was observed. Analysis of thermal curves further suggested a slower rate of melting than the cooling reaction- the very reason for the hysteresis in TERRA mutants. Hence, in contrast to DNA G-quadruplex mutations displaying superimposing nature of cooling and melting curves (except G5A Telo and G5C Telo), base substitutions in RNA G-quadruplex sequence cause disturbances in the equilibrium between its folding and unfolding process by altering the rate of reactions.

A thermodynamic overview across the quartets shows that mutations in TERRA cause drastic decrease in the magnitude of ΔG values from (−) 12.5 kcal/mol to (−) 1−2 kcal/mol, suggesting high degree of destabilization with loss of ΔG value of (−) 10.5−11.5 kcal/mol. ΔG value (−2.2 kcal/mol) of G4C mutant was lowest because of high association rate constant and very low dissociation rate constant. The low magnitude of enthalpy values were major contributors for decreased stability of mutants. Although there was an increase in the entropic values, overall ΔG values was decreased due to enthalpy−entropy compensation. Overall, mutations in TERRA sequence are potent enough to strikingly reduce the stability of the structure. All guanine residues of G-quartets equally contribute to the stability of RNA G-quadruplex. Conversely, ΔG values of Telo DNA mutants, though negative, are relatively low in magnitude upon introducing mutations in the end quartets. The middle quartet mutations have most drastic effect on ΔG values. These findings are in affirmation with the similar results shown by Tomasko et al. for base substitution of guanine with adenine in the middle quartet of the 21 mer human telomeric sequence.[19]

The observed T_m change and Gibb's free energy change upon base substitution in quartets of G-quadruplex reflects steep reduction in the thermal stability of the mutated sequences. This decrease in thermal stability arises due to disturbance in multiple types of molecular interactions such as hydrogen bonding network in the quartet and stacking interactions. First, the Hoogsteen bonding network which actually forms the quartet, is effectively disturbed as base mutation in any of the three quartets is introduced. It disturbs the symmetry of an otherwise well-organized quartet and thereby reduces the stability of the overall structure. Second, base stacking interactions between guanines of the consecutive quartets become distorted. The geometry and alignment between bases is crucial for the base stacking interactions. The contribution of base stacking interactions toward quadruplex stability has been well explained by Marky and co-workers.[43,44] Any change in the base composition of G-quartets causes distortion in these stacks due to altered size, charge and topology of the individual bases and consequently

DOI: 10.1021/acs.jpcb.5b00619
J. Phys. Chem. B XXXX, XXX, XXX−XXX

destabilize the quadruplex. Third, cation co-ordination between quartets is an important factor that contributes to structural stability in G-quadruplex. K^+ ions are known to stabilize quadruplex. Each K^+ ion coordinates with eight O6 atoms of eight guanines to establish a stable cation-dipole environment.[12] Any disturbance in this environment affects the charge distribution and weakens this co-ordination. This disconfigured cation-dipole environment deforms the quartet, thereby rendering the quadruplex thermally less stable.

Mutations in the three G-quartets are equally detrimental for thermal stability of TERRA RNA G-quadruplex irrespective of their position. This reduction is caused by a perturbation in the hydrogen bonding network or in the stacking interaction between the quartets or cation-dipole interactions. The excess favorable enthalpic values of wildtype TERRA compared to its mutants is accredited to stronger stacking of three G-quartets and removal of structured water from TERRA. The highly unfavorable entropy penalty in TERRA is mainly due to uptake and immobilization of counterions and higher ordering of random coil to form G-quadruplex structure. RNA G-quadruplex forms a more compact and less hydrated structure than counterpart DNA G-quadruplex where the 2′ hydroxyl group of ribose sugars makes additional contacts with other groups of nucleotide.[22,32] Because of this compactness and greater intramolecular interactions, each guanine residue of the three quartets contributes to the increased stability of RNA G-quadruplex. Thus, mutation in any of these quartets leads to the destabilization of this secondary structure mainly due to compound effect of distorted hydrogen bonding network in the mutated quartet, disrupted stacking interactions, disconfigured cation−dipole environment, altered intramolecular contacts and modified hydration pattern of RNA G-quadruplex.

Conversely, the extent to which Telo DNA G-quadruplex can be affected by guanine mutation is position dependent. A mutation in either of the external quartets in telo DNA deforms only one guanine−guanine stack and has less pronounced effect, while a mutation in the middle quartet causes widespread destabilization due to extension of disturbance to all three quartets. Lee and Kim in their study with mutated human telomeric quadruplex have shown that thymine mutations destabilize the quadruplex structure and have discussed the role of cation coordination.[11] Tomasko et al. have also provided a similar explanation for their results.[6] Moreover, due to the absence of the 2′-hydroxyl group in its deoxyribose sugar, high intramolecular interactions do not exist in DNA G-quadruplex.

In view to understand the overall effect of mutations in RNA G-quadruplex on ligand binding, a comprehensive comparative analysis of TmPyP4 binding to TERRA mutants was also conducted. TmPyP4 is a known ligand selective for G-quadruplex. The planar arrangement of the aromatic rings in TmPyP4 is known to aid the stacking interaction with the quartets at the ends of G-quadruplex. We characterized the binding capabilities of TmPyP4 to different G-quadruplexes with varying mutations using circular dichroism titrations and isothermal titration calorimetry experiments.

Changes in the CD signals of mutants upon titrating it against TmPyP4 clearly demonstrates that TmPyP4 binds to G-quadruplex despite base substitutions. Curvature in the plots of changes in intensity of CD signals versus TmPyP4 concentration shows existence of two binding sites for TmPyP4 in the sequences. However, the CD signals' intensity decreased with the increasing concentration of TmPyP4 in TERRA and its mutants. A similar decrease in CD signals upon telo DNA−porphyrin interaction was reported earlier by the Giancola group where importance of conformational changes in telo DNA upon TmPyP4 binding was highlighted.[45]

For the better understanding of the thermodynamics and stochiometry of TmPyP4 binding to TERRA and mutants, isothermal titration calorimetry was performed. ITC thermograms also showed two binding modes of TmPyP4 at two independent sites of TERRA G-quadruplex. This is concordance with previous reports.[22,46] Crystal structure of telo DNA quadruplex-TmPyP4 showed two binding modes at independent sites at TmPyP4/G-quadruplex ratio from 1:1 to 5:1.[47] The first binding refers to strong stacking interactions and second binding is represented by weak external binding mainly to the loops. Arora et al. illustrated various schemes of binding of TmPyP4 to G-quadruplex.[46] In TERRA RNA G-quadruplex with parallel topology, the strong binding mode with K_a of 10^8 M^{-1} results from stacking interactions of TmPyP4 to the end quartets of G-quadruplex. The absence of diagonal and lateral loops strengthens the stacking interactions with the end quartets in RNA G-quadruplex with parallel topology. All TERRA mutants displayed moderate changes in ITC profile of wildtype TERRA, with changes similar in most cases. Although mutations in G-quartets made TmPyP4 binding to RNA G-quadruplex enthalpically highly favorable and entropically unfavorable, they demonstrated similar ΔG values as wildtype. What is more, most mutations do not affect TmPyP4 binding by displaying similar binding affinity at first and second binding site. In other wods, TmPyP4 was unable to selectively discriminate between wildtype and mutant RNA G-quadruplexes harboring mutations in the G-quartets.

To summarize, our findings in essence suggest that the most extensive damage to RNA G-quadruplex structure is brought about by changes in the G-quartet. The entire thermodynamic profile suggests that modification in any of the three G-quartets is equally responsible for decreased stability of RNA G-quadruplex. Moreover, the sequence rules pertaining to RNA G-quadruplex does not completely hold true for DNA G-quadruplex and vice versa. Unlike RNA G-quadruplex, the propensity of formation of DNA G-quadruplex with the middle quartet modified is less than either of the other two quartets modified. In all cases, it has been noteworthy that uracil appears to have a similar damaging effect on quadruplex integrity as does adenine and cytosines.

CONCLUSION

Our study presents the impact of base changes on RNA G-quadruplex stability. We have undertaken base changes in three quartets with all possible single base substitutions. The investigation impinges on the findings of Mergny and co-workers where they demonstrate using base substitutions that indeed guanines are the quartet's best friends, providing conditions most conducive to quadruplex formation.[48] More importantly, here we show that the mutations in any of three G-quartets is evenly harmful for the stability of RNA G-quadruplex whereas base substitutions particularly in the middle quartet are most detrimental to the integrity of the DNA G-quadruplex structure. This *in vitro* study hints at the relevance of such a phenomenon of altered structural identity owing to single base changes. The binding behavior of ligand TmPyP4 to mutated RNA G-quadruplex further illustrates the unaltered trans factor activity upon binding to these modified secondary structure. A genome wide study across a population set can give meaningful insights about how such polymorphism

DOI: 10.1021/acs.jpcb.5b00619
J. Phys. Chem. B XXXX, XXX, XXX−XXX

in the population may be actively affecting differential molecular recognition and function possibly leading to phenotypic manifestations.[49]

The single nucleotide polymorphisms shall logically hold true for other RNA quadruplex forming sequences also. The present investigation entails *in vitro* aspects of single base mutations in the telomeric RNA sequences alone. Hence this study unfolds a new dimension in G quadruplex research where minor variations in nucleotide sequences comprising G-quartets impact the overall stability of RNA G-quadruplex. More such studies are desirable before establishing G-quadruplexes as suitable targets for therapeutic intervention, also necessitating genotyping of the subjects for therapy. Additionally, more such studies comprising combinations of such mutations shall be instrumental in predicting G-quadruplex stability and aid in understanding the structure governed complexity of the genome and transcriptome.

■ ASSOCIATED CONTENT

Supporting Information

Table S1, providing kinetic and thermodynamic parameters obtained for mutant RNA oligonucleotides—G4A TERRA, G4C TERRA and G4U TERRA from UV melting studies performed at the rate of 0.5 °C/min, Tables S2 and S3, giving details about Telo DNA and mutant sequences and thermodynamic parameters upon UV melting studies, Figures S1 and S2 showing UV melting and CD spectra of Telo DNA and its mutants, and Figures S3 and S4, depicting CD profile and ITC baseline corrected experimental data for porphyrin binding with TERRA and its mutants. This material is available free of charge via the Internet at http://pubs.acs.org.

■ AUTHOR INFORMATION

Corresponding Author

*(S.M.) Telephone: +91 11 27666156. Fax: +91 11 27667437. E-mail: souvik@igib.res.in.

Funding

This work was supported by Project BSC0123 (Project: Genome Dynamics in Cellular Organization, Differentiation and Enantiostasis) from the Council of Scientific and Industrial Research (CSIR), Government of India, and by the Swarnajayanti project to S.M. from the Department of Science and Technology (DST), Government of India.

Notes

The authors declare no competing financial interest.

■ REFERENCES

(1) Gellert, M.; Lipsett, M. N.; Davies, D. R. Helix Formation by Guanylic Acid. *Proc. Natl. Acad. Sci. U.S.A.* **1962**, *48*, 2013−2018.

(2) Huppert, J. L.; Balasubramanian, S. Prevalence of Quadruplexes in the Human Genome. *Nucleic Acids Res.* **2005**, *33*, 2908−2916.

(3) Huppert, J. L.; Bugaut, A.; Kumari, S.; Balasubramanian, S. G-Quadruplexes: The Beginning and End of Utrs. *Nucleic Acids Res.* **2008**, *36*, 6260−6268.

(4) Jayaraj, G. G.; Pandey, S.; Scaria, V.; Maiti, S. Potential G-Quadruplexes in the Human Long Non-Coding Transcriptome. *RNA Biol.* **2012**, *9*, 81−86.

(5) Guo, Q.; Lu, M.; Kallenbach, N. R. Effect of Thymine Tract Length on the Structure and Stability of Model Telomeric Sequences. *Biochemistry* **1993**, *32*, 3596−3603.

(6) Risitano, A.; Fox, K. R. The Stability of Intramolecular DNA Quadruplexes with Extended Loops Forming Inter- and Intra-Loop Duplexes. *Org. Biomol Chem.* **2003**, *1*, 1852−1855.

(7) Hazel, P.; Huppert, J.; Balasubramanian, S.; Neidle, S. Loop-Length-Dependent Folding of G-Quadruplexes. *J. Am. Chem. Soc.* **2004**, *126*, 16405−16415.

(8) Risitano, A.; Fox, K. R. Influence of Loop Size on the Stability of Intramolecular DNA Quadruplexes. *Nucleic Acids Res.* **2004**, *32*, 2598−2606.

(9) Cevec, M.; Plavec, J. Role of Loop Residues and Cations on the Formation and Stability of Dimeric DNA G-Quadruplexes. *Biochemistry* **2005**, *44*, 15238−15246.

(10) Guedin, A.; De Cian, A.; Gros, J.; Lacroix, L.; Mergny, J. L. Sequence Effects in Single-Base Loops for Quadruplexes. *Biochimie* **2008**, *90*, 686−696.

(11) Kumar, N.; Sahoo, B.; Varun, K. A.; Maiti, S. Effect of Loop Length Variation on Quadruplex-Watson Crick Duplex Competition. *Nucleic Acids Res.* **2008**, *36*, 4433−4442.

(12) Arora, A.; Maiti, S. Stability and Molecular Recognition of Quadruplexes with Different Loop Length in the Absence and Presence of Molecular Crowding Agents. *J. Phys. Chem. B* **2009**, *113*, 8784−8792.

(13) Olsen, C. M.; Marky, L. A. Energetic and Hydration Contributions of the Removal of Methyl Groups from Thymine to Form Uracil in G-Quadruplexes. *J. Phys. Chem. B* **2009**, *113*, 9−11.

(14) Guedin, A.; Alberti, P.; Mergny, J. L. Stability of Intramolecular Quadruplexes: Sequence Effects in the Central Loop. *Nucleic Acids Res.* **2009**, *37*, 5559−5567.

(15) Rachwal, P. A.; Brown, T.; Fox, K. R. Sequence Effects of Single Base Loops in Intramolecular Quadruplex DNA. *FEBS Lett.* **2007**, *581*, 1657−1660.

(16) Pandey, S.; Agarwala, P.; Maiti, S. Effect of Loops and G-Quartets on the Stability of RNA G-Quadruplexes. *J. Phys. Chem. B* **2013**, *117*, 6896−6905.

(17) Zhang, A. Y.; Bugaut, A.; Balasubramanian, S. A Sequence-Independent Analysis of the Loop Length Dependence of Intramolecular RNA G-Quadruplex Stability and Topology. *Biochemistry* **2011**, *50*, 7251−7258.

(18) Kwok, C. K.; Sherlock, M. E.; Bevilacqua, P. C. Effect of Loop Sequence and Loop Length on the Intrinsic Fluorescence of G-Quadruplexes. *Biochemistry* **2013**, *52*, 3019−3021.

(19) Tomasko, M.; Vorlickova, M.; Sagi, J. Substitution of Adenine for Guanine in the Quadruplex-Forming Human Telomere DNA Sequence G(3)(T(2)Ag(3))(3). *Biochimie* **2009**, *91*, 171−179.

(20) Pedroso, I. M.; Duarte, L. F.; Yanez, G.; Burkewitz, K.; Fletcher, T. M. Sequence Specificity of Inter- and Intramolecular G-Quadruplex Formation by Human Telomeric DNA. *Biopolymers* **2007**, *87*, 74−84.

(21) Lee, J. Y.; Kim, D. S. Dramatic Effect of Single-Base Mutation on the Conformational Dynamics of Human Telomeric G-Quadruplex. *Nucleic Acids Res.* **2009**, *37*, 3625−3634.

(22) Arora, A.; Maiti, S. Differential Biophysical Behavior of Human Telomeric RNA and DNA Quadruplex. *J. Phys. Chem. B* **2009**, *113*, 10515−10520.

(23) Sacca, B.; Lacroix, L.; Mergny, J. L. The Effect of Chemical Modifications on the Thermal Stability of Different G-Quadruplex-Forming Oligonucleotides. *Nucleic Acids Res.* **2005**, *33*, 1182−1192.

(24) Neidle, S.; Parkinson, G. N. The Structure of Telomeric DNA. *Curr. Opin Struct Biol.* **2003**, *13*, 275−283.

(25) Gavathiotis, E.; Searle, M. S. Structure of the Parallel-Stranded DNA Quadruplex D(Ttagggt)4 Containing the Human Telomeric Repeat: Evidence for a-Tetrad Formation from Nmr and Molecular Dynamics Simulations. *Org. Biomol Chem.* **2003**, *1*, 1650−1656.

(26) Ambrus, A.; Chen, D.; Dai, J.; Bialis, T.; Jones, R. A.; Yang, D. Human Telomeric Sequence Forms a Hybrid-Type Intramolecular G-Quadruplex Structure with Mixed Parallel/Antiparallel Strands in Potassium Solution. *Nucleic Acids Res.* **2006**, *34*, 2723−2735.

(27) Burge, S.; Parkinson, G. N.; Hazel, P.; Todd, A. K.; Neidle, S. Quadruplex DNA: Sequence, Topology and Structure. *Nucleic Acids Res.* **2006**, *34*, 5402−5415.

(28) Dai, J.; Punchihewa, C.; Ambrus, A.; Chen, D.; Jones, R. A.; Yang, D. Structure of the Intramolecular Human Telomeric G-

DOI: 10.1021/acs.jpcb.5b00619
J. Phys. Chem. B XXXX, XXX, XXX−XXX

Quadruplex in Potassium Solution: A Novel Adenine Triple Formation. *Nucleic Acids Res.* **2007**, *35*, 2440−2450.
(29) Neidle, S.; Parkinson, G. N. Quadruplex DNA Crystal Structures and Drug Design. *Biochimie* **2008**, *90*, 1184−1196.
(30) Xu, Y.; Kaminaga, K.; Komiyama, M. G-Quadruplex Formation by Human Telomeric Repeats-Containing RNA in Na+ Solution. *J. Am. Chem. Soc.* **2008**, *130*, 11179−11184.
(31) Martadinata, H.; Phan, A. T. Structure of Propeller-Type Parallel-Stranded RNA G-Quadruplexes, Formed by Human Telomeric RNA Sequences in K+ Solution. *J. Am. Chem. Soc.* **2009**, *131*, 2570−2578.
(32) Collie, G. W.; Haider, S. M.; Neidle, S.; Parkinson, G. N. A Crystallographic and Modelling Study of a Human Telomeric RNA (Terra) Quadruplex. *Nucleic Acids Res.* **2010**, *38*, 5569−5580.
(33) Phan, A. T. Human Telomeric G-Quadruplex: Structures of DNA and RNA Sequences. *FEBS J.* **2010**, *277*, 1107−1117.
(34) Parkinson, G. N.; Lee, M. P.; Neidle, S. Crystal Structure of Parallel Quadruplexes from Human Telomeric DNA. *Nature* **2002**, *417*, 876−880.
(35) Cantor, C. R.; Warshaw, M. M.; Shapiro, H. Oligonucleotide Interactions. 3. Circular Dichroism Studies of the Conformation of Deoxyoligonucleotides. *Biopolymers* **1970**, *9*, 1059−1077.
(36) Hatzakis, E.; Okamoto, K.; Yang, D. Thermodynamic Stability and Folding Kinetics of the Major G-Quadruplex and Its Loop Isomers Formed in the Nuclease Hypersensitive Element in the Human C-Myc Promoter: Effect of Loops and Flanking Segments on the Stability of Parallel-Stranded Intramolecular G-Quadruplexes. *Biochemistry* **2010**, *49*, 9152−9160.
(37) Indyk, L.; Fisher, H. F. Theoretical Aspects of Isothermal Titration Calorimetry. *Methods Enzymol* **1998**, *295*, 350−364.
(38) Pierce, M. M.; Raman, C. S.; Nall, B. T. Isothermal Titration Calorimetry of Protein-Protein Interactions. *Methods* **1999**, *19*, 213−221.
(39) Mergny, J. L.; Phan, A. T.; Lacroix, L. Following G-Quartet Formation by Uv-Spectroscopy. *FEBS Lett.* **1998**, *435*, 74−78.
(40) Rougee, M.; Faucon, B.; Mergny, J. L.; Barcelo, F.; Giovannangeli, C.; Garestier, T.; Helene, C. Kinetics and Thermodynamics of Triple-Helix Formation: Effects of Ionic Strength and Mismatches. *Biochemistry* **1992**, *31*, 9269−9278.
(41) Brown, N. M.; Rachwal, P. A.; Brown, T.; Fox, K. R. Exceptionally Slow Kinetics of the Intramolecular Quadruplex Formed by the Oxytricha Telomeric Repeat. *Org. Biomol Chem.* **2005**, *3*, 4153−4157.
(42) Mergny, J. L.; De Cian, A.; Ghelab, A.; Sacca, B.; Lacroix, L. Kinetics of Tetramolecular Quadruplexes. *Nucleic Acids Res.* **2005**, *33*, 81−94.
(43) Olsen, C. M.; Gmeiner, W. H.; Marky, L. A. Unfolding of G-Quadruplexes: Energetic, and Ion and Water Contributions of G-Quartet Stacking. *J. Phys. Chem. B* **2006**, *110*, 6962−6969.
(44) Lee, H. T.; Olsen, C. M.; Waters, L.; Sukup, H.; Marky, L. A. Thermodynamic Contributions of the Reactions of DNA Intramolecular Structures with Their Complementary Strands. *Biochimie* **2008**, *90*, 1052−1063.
(45) Martino, L.; Pagano, B.; Fotticchia, I.; Neidle, S.; Giancola, C. Shedding Light on the Interaction between Tmpyp4 and Human Telomeric Quadruplexes. *J. Phys. Chem. B* **2009**, *113*, 14779−14786.
(46) Arora, A.; Maiti, S. Effect of Loop Orientation on Quadruplex-Tmpyp4 Interaction. *J. Phys. Chem. B* **2008**, *112*, 8151−8159.
(47) Parkinson, G. N.; Ghosh, R.; Neidle, S. Structural Basis for Binding of Porphyrin to Human Telomeres. *Biochemistry* **2007**, *46*, 2390−2397.
(48) Gros, J.; Rosu, F.; Amrane, S.; De Cian, A.; Gabelica, V.; Lacroix, L.; Mergny, J. L. Guanines Are a Quartet's Best Friend: Impact of Base Substitutions on the Kinetics and Stability of Tetramolecular Quadruplexes. *Nucleic Acids Res.* **2007**, *35*, 3064−3075.
(49) Baral, A.; Kumar, P.; Halder, R.; Mani, P.; Yadav, V. K.; Singh, A.; Das, S. K.; Chowdhury, S. Quadruplex-Single Nucleotide Polymorphisms (Quad-SNP) Influence Gene Expression Difference among Individuals. *Nucleic Acids Res.* **2012**, *40*, 3800−3811.

DOI: 10.1021/acs.jpcb.5b00619
J. Phys. Chem. B XXXX, XXX, XXX−XXX